SYMPOSIUM

Recent Progress in the Physical Principles of Dynamic Ground Self-Righting

Chen Li [ORCID] [1]

Department of Mechanical Engineering, Johns Hopkins University , Baltimore, Maryland 21218, USA

From the symposium "Computational and Physical Models in Research and Teaching to Explore Form–Function Relationships" presented at the annual meeting of the Society for Integrative and Comparative Biology, January 2–6, 2024.

[1]E-mail: chen.li@jhu.edu

Synopsis   Animals and robots must self-right on the ground after overturning. Biology research has described various strategies and motor patterns in many species. Robotics research has devised many strategies. However, we do not well understand the physical principles of how the need to generate mechanical energy to overcome the potential energy barrier governs behavioral strategies and 3D body rotations given the morphology. Here, I review progress on this which I led studying cockroaches self-righting on level, flat, solid, low-friction ground, by integrating biology experiments, robotic modeling, and physics modeling. Animal experiments using three species (Madagascar hissing, American, and discoid cockroaches) found that ground self-righting is strenuous and often requires multiple attempts to succeed. Two species (American and discoid cockroaches) often self-right dynamically, using kinetic energy to overcome the barrier. All three species use and often stochastically transition across diverse strategies. In these strategies, propelling motions are often accompanied by perturbing motions. All three species often display complex yet stereotyped body rotation. They all roll more in successful attempts than in failed ones, which lowers the barrier, as revealed by a simplistic 3D potential energy landscape of a rigid body self-righting. Experiments of an initial robot self-righting via rotation about a fixed axis revealed that the longer and faster appendages push, the more mechanical energy can be gained to overcome the barrier. However, the cockroaches rarely achieve this. To further understand the physical principles of strenuous ground self-righting, we focused on the discoid cockroach's leg-assisted winged self-righting. In this strategy, wings propel against the ground to pitch the body up but are unable to overcome the highest pitch barrier. Meanwhile, legs flail in the air to perturb the body sideways to self-right via rolling. Experiments using a refined robot and an evolving 3D potential energy landscape revealed that, although wing propelling cannot generate sufficient kinetic energy to overcome the highest pitch barrier, it reduces the barrier to allow small kinetic energy from the perturbing legs to probabilistically overcome the barrier to self-right via rolling. Thus, only by combining propelling and perturbing can self-righting be achieved when it is so strenuous; this physical constraint leads to the stereotyped body rotation. Finally, multi-body dynamics simulation and template modeling revealed that the animal's substantial randomness in wing and leg motions helps it, by chance, to find good coordination, which accumulates more mechanical energy to overcome the barrier, thus increasing the likelihood of self-righting.

Introduction

Righting oneself from being upside down on the ground is a prevalent locomotor maneuver that animals must make to survive. Even on level, flat, solid ground with high friction, locomotion can result in overturning. On uneven (Clifton et al. 2023), sloped, or slippery surfaces, overturning is even more likely. Falling during jumping, climbing, or flying, as well as fighting (Mann et al. 2006) and courtship (Willemsen and Hailey 2003), can also lead to overturning. Once overturned, animals must self-right promptly to avoid predation, starvation, and dehydration. Many animals need to self-right even simply after sleep. Similarly, mobile robots can flip over during a diversity of locomotor tasks (Li et al. 2016,

2017). How likely and quickly animals and robots can self-right on the ground is important for their survival or continued and timely operation.

Ground self-righting behavior and motor patterns have been extensively studied in insects, such as cockroaches (Camhi 1977; Reingold and Camhi 1977; Sherman et al. 1977; Zill 1986; Full et al. 1995), beetles (Evans 1972; Frantsevich and Mokrushov 1980; Frantsevich 2004; Sasaki and Nonaka 2016; Bolmin et al. 2017; Zhang et al. 2021), stick insects (Graham 1979), locusts (Faisal and Matheson 2001), stink bugs (Pace and Harris 2021), lanternflies (Bien et al. 2024), and springtails (Brackenbury 1990), as well as in other animals such as crustaceans (Silvey and Silvey 1973; Young et al. 2006), mollusks (Weldon and Hoffman 1979; Hoffman 1980; Zhang et al. 2020), toads (Robins et al. 1998), lizards (Caporale et al. 2019), turtles (Ashe 1970; Stancher et al. 2006; Domokos and Várkonyi 2008; Golubović et al. 2015; Malashichev 2016; Rubin et al. 2018; Ewart et al. 2022), birds (Koppányi and Kleitman 1927), and mammals (Vince 1986; Pellis et al. 1991). Many biological ground self-righting strategies have been described, including (1) using appendages (e.g., legs, wings, tail, antennae, and ventral tube) and neck/head to grasp, pivot, push, pull, or shake (Koppányi and Kleitman 1927; Ashe 1970; Silvey and Silvey 1973; Weldon and Hoffman 1979; Frantsevich and Mokrushov 1980; Hoffman 1980; Vince 1986; Brackenbury 1990; Pellis et al. 1991; Full et al. 1995; Robins et al. 1998; Faisal and Matheson 2001; Frantsevich 2004; Stancher et al. 2006; Young et al. 2006; Domokos and Várkonyi 2008; Golubović et al. 2015; Malashichev 2016; Sasaki and Nonaka 2016; Rubin et al. 2018; Zhang et al. 2020, 2021; Pace and Harris 2021; Ewart et al. 2022; Bien et al. 2024), (2) deforming the body (Camhi 1977; Pellis et al. 1991; Young et al. 2006; Caporale et al. 2019), (3) having a body shape and center of mass (CoM) that makes an upside-down orientation unstable (Várkonyi and Domokos 2006; Domokos and Várkonyi 2008), and (4) jumping with elastic energy storage and release then falling into an upright orientation by chance (Evans 1972; Frantsevich 2004; Bolmin et al. 2017). Different types of appendages and body deformation are often used together (Koppányi and Kleitman 1927; Ashe 1970; Hoffman 1980; Vince 1986; Brackenbury 1990; Pellis et al. 1991; Faisal and Matheson 2001; Stancher et al. 2006; Young et al. 2006; Domokos and Várkonyi 2008; Malashichev 2016; Zhang et al. 2021). These diverse strategies lead to self-righting via diverse body rotations, including pitching, rolling, and diagonal rotations with both pitching and rolling (Silvey and Silvey 1973; Camhi 1977; Weldon and Hoffman 1979; Frantsevich and Mokrushov 1980; Brackenbury

1990; Pellis et al. 1991; Full et al. 1995; Robins et al. 1998; Faisal and Matheson 2001; Frantsevich 2004; Stancher et al. 2006; Young et al. 2006; Domokos and Várkonyi 2008; Malashichev 2016; Sasaki and Nonaka 2016; Rubin et al. 2018; Zhang et al. 2020, 2021; Pace and Harris 2021; Ewart et al. 2022; Bien et al. 2024). Many species use multiple strategies and transition among them to self-right (Ashe 1970; Camhi 1977; Pellis et al. 1991; Frantsevich 2004; Sasaki and Nonaka 2016; Pace and Harris 2021; Zhang et al. 2021; Bien et al. 2024). For robots, a diversity of terrestrial self-righting strategies have also been developed, including all four categories above, as well as having a symmetric body design without an upright orientation (for a brief review, see Li et al. 2016, 2017).

Given these rich descriptions of biological strategies and motor patterns as well as plentiful development of robot strategies, we know relatively little about the physical principles of how the fundamental need to generate mechanical energy (kinetic energy and potential energy) to overcome the potential energy barrier to self-right on the ground governs behavioral strategies and body rotations given the morphology.

Here, I review the major findings from recent studies (Li et al. 2016, 2017, 2019; Xuan and Li 2020a, 2020b; Othayoth and Li 2021) that I led to begin to fill this knowledge gap, focusing on cockroaches and their robophysical models (Aguilar et al. 2016). Our inquiries began with developing a cockroach-inspired robot, which relies on opening its wings to self-right dynamically (Fig. 1) (Li et al. 2016, 2017). Inspired by a 2D potential energy landscape model for turtle ground self-righting (Fig. 2), we tested this initial robot to reveal the physical principles of dynamic ground self-righting via a fixed-axis body rotation to overcome the potential energy barrier (Fig. 3) (Li et al. 2016, 2017). To test whether cockroaches use such simple rotations, we performed animal experiments to quantify how three species of cockroaches use and transition across various self-righting strategies (Figs. 4–6) (Li et al. 2019). We developed a simplistic 3D potential energy landscape model and measured the animals' often complex yet stereotyped 3D body rotations (Figs. 7 and 8) to explain why each species rolls more during successful attempts than failed ones (Li et al. 2019). More interesting questions arose from our animal observations—that ground self-righting is often dynamic (using kinetic energy to overcome the potential energy barrier) yet strenuous, the body rotation is stereotyped, propelling motions are accompanied by perturbing motions, and there is substantial randomness in these motions. To better understand the physical principles governing these, we then focused on the discoid cockroach's strenuous, leg-assisted winged self-righting as a model system (Fig. 9).

By combining robophysical modeling and evolving potential energy landscape modeling with a refined robot (Figs. 10 and 11) (Othayoth and Li 2021), multi-body dynamics simulation (Fig. 12) (Xuan and Li 2020b), and template modeling (Fig. 13) (Xuan and Li 2020a), we elucidated the physical constraints that lead to stereotyped body rotation, and how and why the cooperation, coordination, and substantial randomness in the motions of propelling wings and perturbing legs contribute to successful self-righting. This brief review focuses on threading together the major approaches and findings of these studies. For a deeper dive into the focus, motivation, methods, results, implications, and limitations of each study, please refer to the original research papers.

Before reviewing our work, we note that the physical principles of ground self-righting dominated by ground reaction forces differ from aerial and underwater self-righting dominated by different forces. When aerodynamic forces are negligible, aerial self-righting is governed by the conservation of angular momentum, and animals can rotate their appendages to induce counter-rotations of the body to self-right (e.g., Jusufi et al. 2008). When aerodynamic forces dominate, animals can control their aerodynamic surfaces to generate rotating torques to self-right in the air (e.g., Zeng et al. 2017). The physical principles of aerial self-righting have been well understood; for a comprehensive review, see Ortega-Jimenez et al. (2023). Similarly, underwater self-righting that predominantly uses hydrodynamic forces, with little substrate interaction (e.g., Davis 1968), should have physical principles more similar to aerial self-righting in the limit when aerodynamic forces dominate (e.g., Zeng et al. 2017).
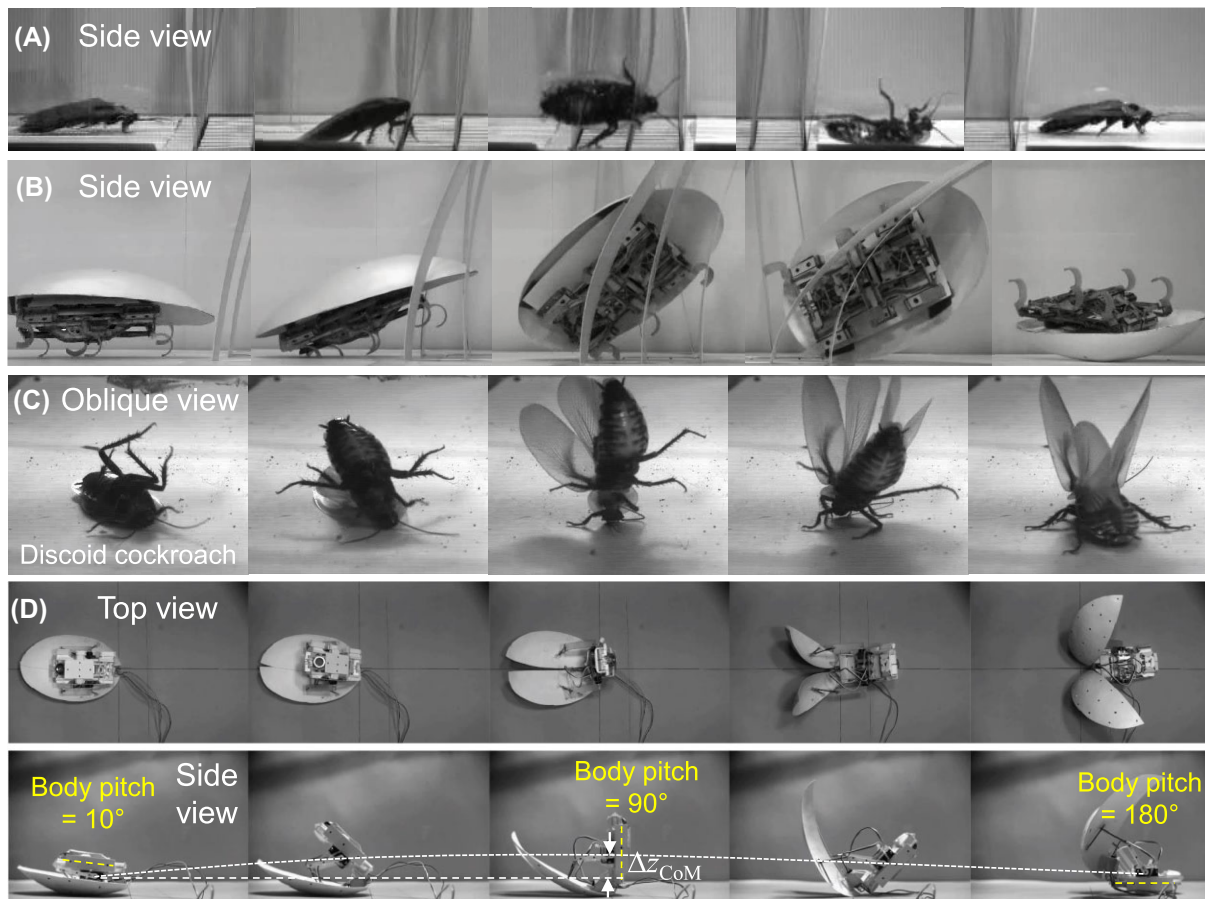

Fig. 1 Study of cockroach and robot traversing cluttered obstacles led to study of cockroach and robot ground self-righting. Adapted from Li et al. (2017). (**A**) A discoid cockroach traverses cluttered, grass-like beam obstacles, during which its wings are folded against the body as a rounded ellipsoidal "shell" to facilitate body rolling into obstacle gaps. It flips over upon exiting the obstacles and quickly rights itself. (**B**) A small six-legged robot uses a cockroach-inspired rounded shell to traverse cluttered obstacles. However, when it over-rolls and flips over, it cannot self-right. (**C**) The cockroach self-rights by opening and pushing its wings against the ground to pitch and roll its body. (**D**) The robot with the rounded shell cut into two wings, which open to push against the ground, to self-right via pure body pitching. Change in body pitch is shown by yellow dashed lines. White dashed curve shows that CoM height increases by Δz_{CoM} (defined by arrows) from an upside-down orientation (leftmost) to the highest CoM orientation (middle), then decreases. Potential energy barrier is $\Delta E_{potential} = mg\Delta z_{CoM}$, where m is total body mass and g is gravitational acceleration. Adapted from Li et al. (2017).

However, underwater ground self-righting that largely relies on interaction with the bottom substrates (Silvey and Silvey 1973; Weldon and Hoffman 1979; Hoffman 1980; Young et al. 2006; Zhang et al. 2020) should be governed by similar principles as ground self-righting, except that the larger hydrostatic and hydrodynamic forces need to be taken into account (whereas the buoyant and drag forces in the air are negligible during ground self-righting).

How it all started

In an earlier study of how insects traverse cluttered, grass-like beam obstacles, we discovered that the discoid cockroach's rounded body shape helps it roll into narrow gaps between obstacles to traverse (Fig. 1A) (Li et al. 2015). A cockroach-inspired rounded shell enabled a legged robot to roll its body into obstacle gaps to traverse similar cluttered obstacles (Fig. 1B). However, the robot sometimes over rolls and flips over, and it gets stuck (Fig. 1B), whereas the cockroach sometimes flips over, too, but can recover (Fig. 1A) by using its wings to push against the ground (Fig. 1C). This led us to develop the robot's rounded shell into two actuated wings that push against the ground to self-right via body pitching (Fig. 1D) (Li et al. 2016, 2017). In this process, I became interested in understanding the physical principles of ground self-righting.

Inspiration from modeling of turtle ground self-righting

To self-right on the ground, an animal or robot must change its body orientation from upside down to upright (e.g., change body pitch from ∼0° to 180°, Fig. 1D, bottom; change body roll from 0° to 180°, Fig. 2A, bottom), which requires overcoming a gravitational potential energy barrier (Figs. 1D and 2A). A previous study used a 2D potential energy landscape to model turtles self-righting via body rolling in the transverse plane (Fig. 2) (Domokos and Várkonyi 2008). It well explained why turtles of highly domed shells with a low (or even diminished) barrier can simply use passive body rolling complemented by leg and neck motions to self-right (Fig. 2B), whereas turtles with flatter shells leading to a higher barrier must more vigorously use their legs and neck to push against the ground to self-right (Fig. 2A). A similar potential energy landscape framework has also been established for motion planning of robots using an appendage to self-right quasi-statically on sloped planar surfaces in the sagittal plane (Kessens et al. 2012).

Principles of ground self-righting with single-axis body rotations

To understand the physical principles of ground self-righting, we first systematically studied our initial cockroach-inspired robot (Fig. 1D) (Li et al. 2016, 2017). Because its body is longest in the longitudinal direction, when the robot self-rights via body pitching, it has to overcome the largest potential energy barrier. We varied the wing opening amplitude Θ_{wing} and speed ω_{wing} (how much and how fast the wings open) to test how they affect the robot's ability to overcome this largest barrier (Fig. 3). The more and faster the wings open, the more likely the robot is to self-right (Fig. 3A and B), and the shorter the time it takes (Fig. 3A and C).

This initial robot experiment revealed intuitive physical principles of ground self-righting using appendages to generate a simple body rotation about a fixed axis:
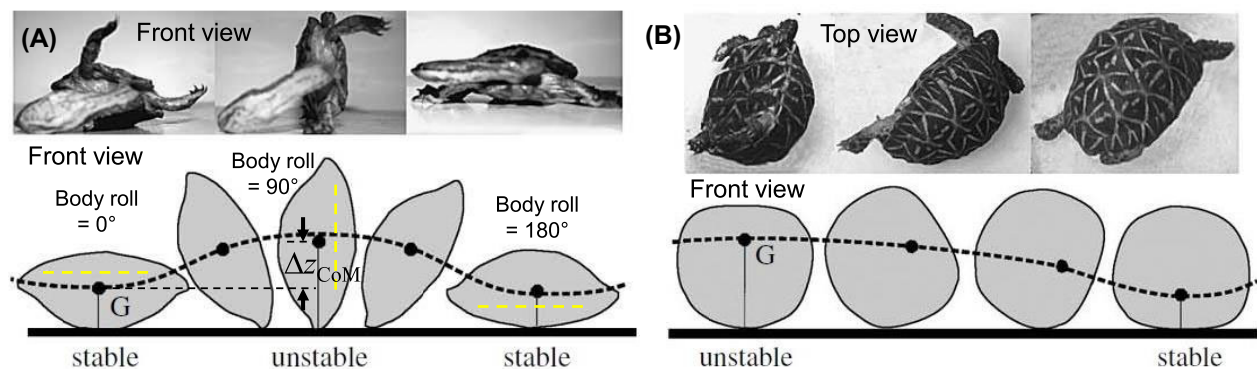
Fig. 2 Potential energy landscape for turtle ground self-righting in 2D via body rolling. **(A)** Potential energy barrier, $\Delta E_{\text{potential}} = mg\Delta z_{\text{CoM}}$, is high for turtles with a flatter shell. Black dashed curve shows that CoM height increases by Δz_{CoM} (defined by black arrows) from an upside-down orientation (leftmost) to the highest CoM orientation (middle), then decreases. Potential energy barrier is $\Delta E_{\text{potential}} = mg\Delta z_{\text{CoM}}$, where m is total body mass and g is gravitational acceleration. Change in body roll is shown by yellow dashed lines. **(B)** Potential energy barrier to self-right diminishes for turtles with a highly domed shell and low CoM when upright. Adapted from Domokos and Várkonyi (2008).
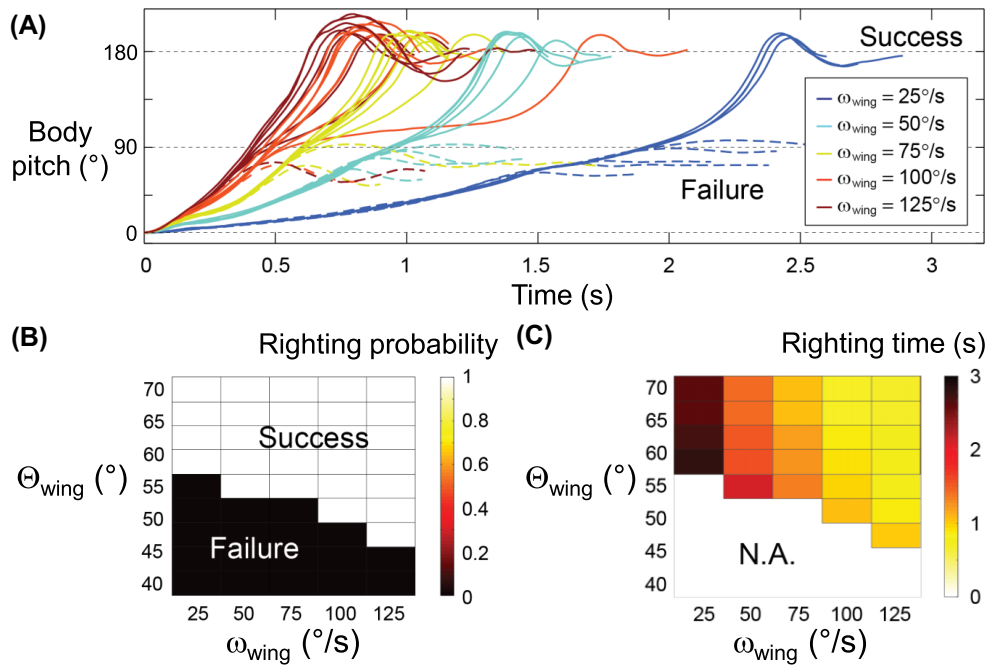
Fig. 3 How appendage pushing magnitude and speed affect self-righting via a simple rotation about a fixed axis, from experiments using the initial robot (Fig. 1D). (**A**) Body pitch as a function of time for a wide range of wing opening amplitude Θ_{wing} and speed ω_{wing}. Each curve of the same color shows one of the three trials that uses the same ω_{wing} (value in legend) but a different Θ_{wing}. Solid and dashed curves show successful and failed trials, respectively. (**B** and **C**) Righting probability and average righting time as a function of Θ_{wing} and ω_{wing}. Adapted from Li et al. (2017).

The longer and faster the appendages propel against the ground, the more mechanical energy can be gained to overcome the barrier to self-right on the ground (Li et al. 2016, 2017). However, do animals always use such simple body rotations to self-right? If not, what are the physical principles that govern more complex self-righting via 3D body rotations? Can we understand these principles using a potential energy landscape approach?

Ground self-righting may require multiple attempts

To explore these questions, we studied the Madagascar hissing, American, and discoid cockroaches self-righting on a level, flat, solid, low-friction surface (Li et al. 2019). All three species always self-right if given sufficient time (near 100% probability within 30 s, Fig. 4A, white). However, although in some trials the animals can self-right upon the first attempt, in other trials
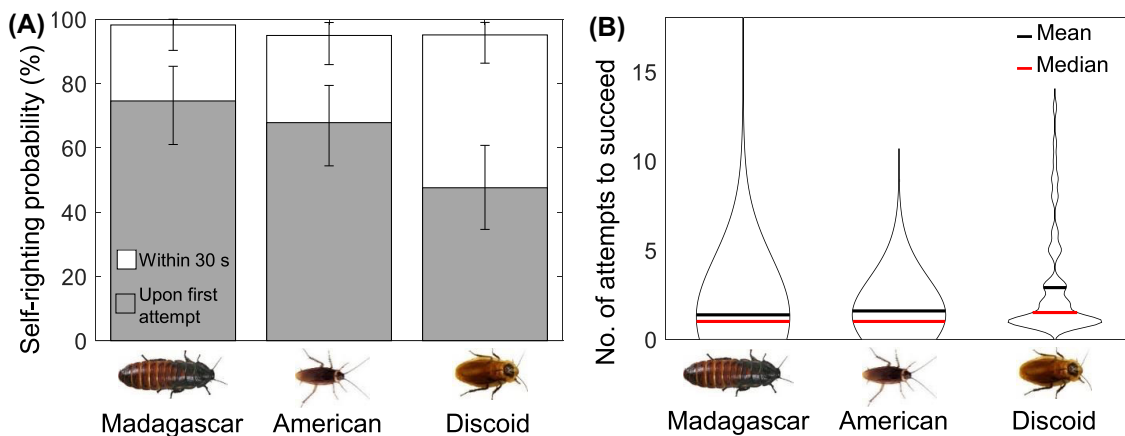

Fig. 4 Self-righting performance. (**A**) Self-righting probability within 30 s (white) and on the first attempt (gray). Error bars represent 95% confidence interval. (**B**) Violin plots of the number of attempts required to achieve self-righting. Width of graph shows the relative frequency of the data along the y-axis. Black and red lines show mean and median for each species. Adapted from Li et al. (2019).

they struggle, requiring multiple attempts to self-right (Figs. 4B; Fig. 4A, gray). Although they can self-right within a short time (∼1 s) if the first attempt is successful, when multiple attempts are needed, self-righting can take much longer (up to ∼10 s).

Cockroaches use and transition across diverse strategies and often self-right dynamically

All three species attempt to use more than one strategy to self-right (e.g., Fig. 5) and often transition across them (Fig. 6) (Li et al. 2019). The Madagascar hissing cockroach often hyperextends its body into an arch to roll onto one side, followed by leg scrubbing against the ground (Fig. 5A), which almost always leads to successful self-righting eventually (Fig. 6A, yellow). Occasionally, it twists the body in an attempt to find objects the legs can grasp onto, but this never leads to successful self-righting (Fig. 6A, green). Both the American and discoid cockroaches can use two strategies (Fig. 6B and C) that can lead to successful self-righting, with wings (Fig. 5B and D) or legs (Fig. 5C and E) as the main propelling appendages to push against the ground, respectively. Notably, both the American and discoid cockroaches often self-right dynamically, by gaining sufficient pitch and roll kinetic energy from wings or legs pushing against the ground to overcome the potential energy barrier. The American cockroach also very occasionally flaps its wings, which always fails in righting itself (Fig. 6B, cyan). All species sometimes enter quiescence without apparent movement (Fig. 6A–C, white oval).
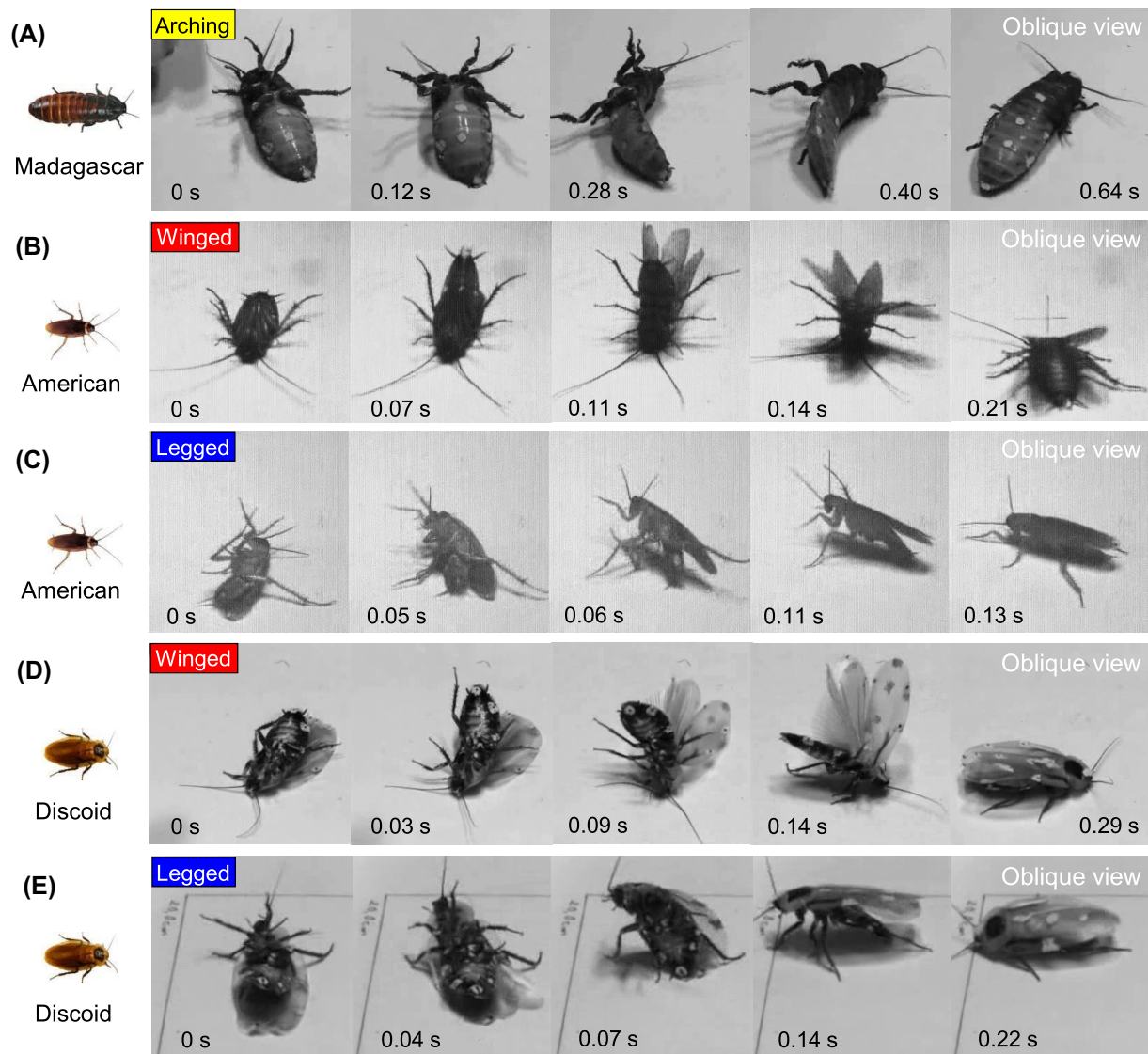

Fig. 5 Self-righting strategies that lead to success. (**A**) Madagascar hissing cockroach using body arching to self-right. (**B** and **C**) American cockroach using wings or legs to self-right. (**D** and **E**) Discoid cockroach using wings or legs to self-right. Adapted from Li et al. (2019).
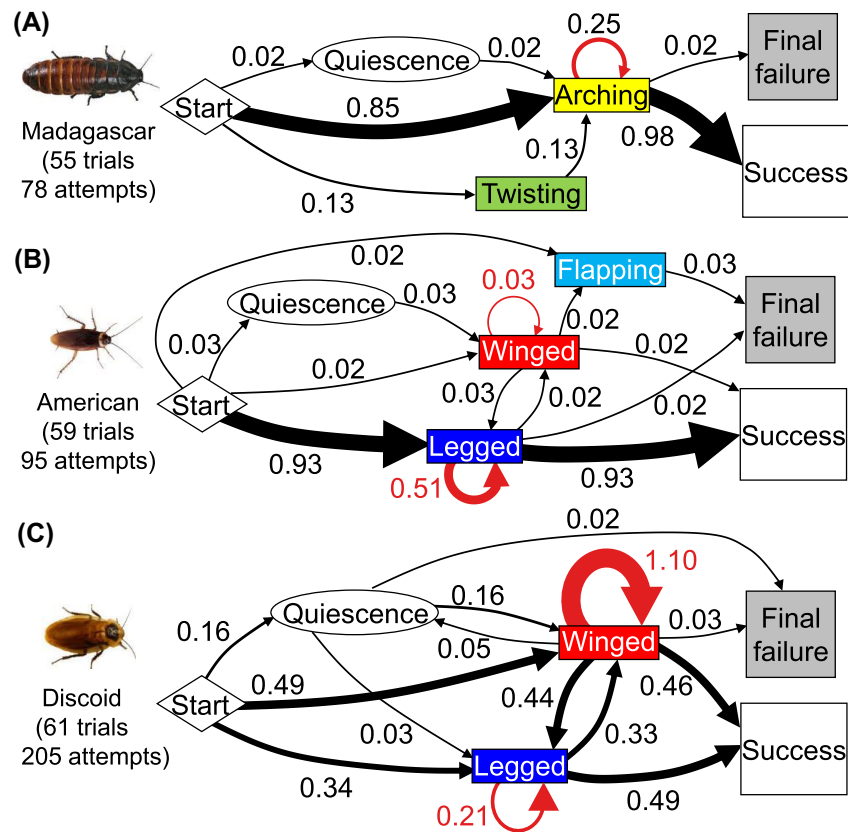
Fig. 6 Self-righting locomotor transition ethograms. (**A**) Madagascar hissing cockroach. (**B**) American cockroach. (**C**) Discoid cockroach. Arrow widths are proportional to transition relative frequencies, with values shown by numbers. Relative frequency is defined as the ratio of the number of occurrences of each transition to the total number of trials for each species. The sum of relative frequencies out of each node equals that into the node, except for start with a sum of 1 going out, and success and final failure with a sum of 1 into both together. (Final failure occurs in some trials, when the animal is able to self-right before the trial concludes at 30 s; in other trials, the animal can fail multiple attempts but eventually succeeds in self-righting.) Red arrows and numbers show probabilities of self-transitions (into the same node) and represent the average number of times of continuing the same strategy during each trial. A self-transition probability greater than one means that, on average, it occurred more than once for each trial. Only the strategies that can lead to successful self-righting on the level, flat, solid, low-friction ground are shown in Fig. 5. Adapted from Li et al. (2019).

Propelling motions are accompanied by perturbing motions with substantial randomness

The winged and legged strategies (Fig. 5C–E) often involve using more than a single type of appendage or even deforming the body (Li et al. 2019). During winged self-righting, the discoid cockroach also flexes and twists the abdomen, flails the legs, and/or scrapes the legs against the ground (Fig. 5D). During legged self-righting, both the American and discoid cockroaches also flex and/or twist the abdomen (Fig. 5C and E). In other words, the primary propelling appendages (wings in the winged strategy; legs in the legged strategy) are accompanied by assisting motions by other appendages or body deformation, which provides additional perturbations.

In addition, both the propelling and perturbing motions are quite erratic, with large variations in the direction, magnitude, frequency, and coordination (phase offset between various motions) from attempt to attempt (Li et al. 2019). The randomness in these motions is much larger than that in the highly rhythmic leg oscillations during walking (Watson and Ritzmann 1997) and running (Full and Tu 1990). Previous neurophysiological studies also showed that leg activation patterns during ground self-righting are more random than during walking (Sherman et al. 1977; Zill 1986).

Stochasticity and stereotypy of use of self-righting strategy

In any single trial, it is stochastic which strategy an animal will use or transition to, or if it will continue using the same strategy, over each attempt. However, averaging over large numbers of trials (see sample size in Fig. 6), the behavioral pattern of each species using strategies is stereotyped (Fig. 6) (Li et al. 2019). Here, behavioral stereotypy means that the actual observed
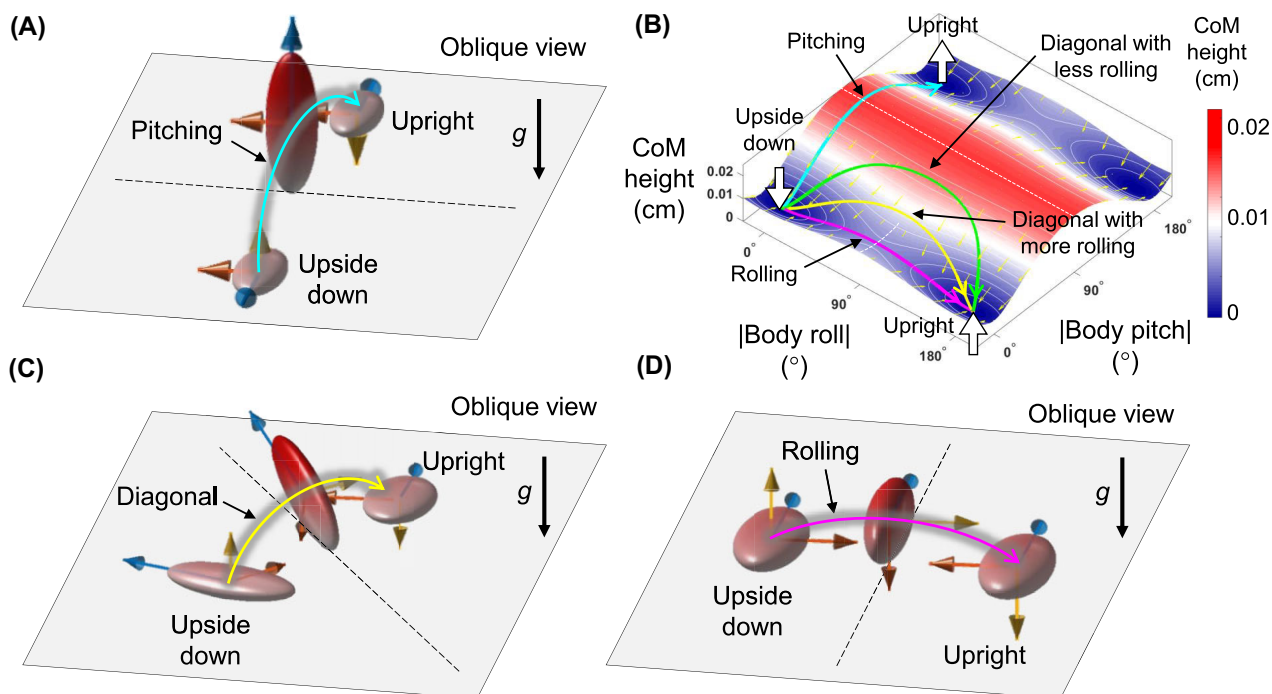
Fig. 7 Simplistic 3D potential energy landscape of an ellipsoidal rigid body. (**A, C,** and **D**) An ellipsoid approximating the animal body in contact with the ground, either pitching (**A**), rolling (**D**), or rotating diagonally, with simultaneous pitching and rolling (**C**). (**A–C**) all show simple rotations about a fixed axis (dashed line) within the horizontal ground plane. Actual rotation of the animal body may be about a time-varying axis. Red, blue, and yellow arrows on each ellipsoidal body show its three major axes to illustrate body rotation. Vector *g* shows the direction of gravity. (**B**) Potential energy landscape, shown as CoM height as a function of body pitch and roll, using Euler angles with yaw-pitch-roll convention. We use absolute values of body pitch and roll, considering symmetry of the ellipsoid. Downward and upward white arrows indicate upside-down and upright body orientations, respectively. Cyan, green, yellow, and magenta curves with arrows are representative trajectories for pure pitching, two different diagonal rotations, and pure rolling, each about its own fixed axis in the horizontal plane, to illustrate the decrease of potential energy barrier with more body rolling. White curves on the landscape are iso-height contours. Small yellow arrows on the landscape are gradients. Model results shown are using the discoid cockroach's body dimensions as an example. Adapted from Li et al. (2019).

behavior is a small fraction of a large number of possibilities (see Berman 2018; Brown and de Bivort 2018). Specifically, both the Madagascar hissing and American cockroaches predominantly rely on a single strategy (body arching and legged strategy, respectively) to self-right (Fig. 6A and B). By contrast, the discoid cockroach has a more balanced use of two strategies (winged and legged) (Fig. 6C).

Simplistic 3D potential energy landscape reveals that more body rolling is advantageous

We observed that the cockroaches' body rotations during ground self-righting are rarely about a fixed axis in the pitch-roll space, but often complex and non-planar (e.g., Fig. 5B–E). Thus, to understand the physical principles, we needed to expand the potential energy landscape approach into three dimensions. As a first step, we developed a simplistic 3D potential energy landscape (Li et al. 2019) (Fig. 7). By approximating each cockroach species' body shape with an ellipsoid of sim-

ilar dimensions, we calculated its potential energy as a function of body pitch and roll using Euler angles (Fig. 7B). These animals' body length is greater than their body width, which is greater than body height. Thus, self-righting by pure body pitching overcomes the highest potential energy barrier (Fig. 7A and B, cyan), and self-righting by pure body rolling overcomes the lowest barrier (Fig. 7B and D, magenta). Self-righting using body rotations with simultaneous pitching and rolling overcomes an intermediate barrier (e.g., Fig. 7B and C, green, yellow), and the more it rolls, the lower the barrier becomes (Fig. 7B, green vs. yellow). Pure body yawing without pitching or rolling cannot raise the CoM.

Self-righting body rotations can be complex and are stereotyped

We then examined each species' body pitch and roll at three stages of each attempt (start, highest CoM orientation, and end) on the simplistic 3D potential
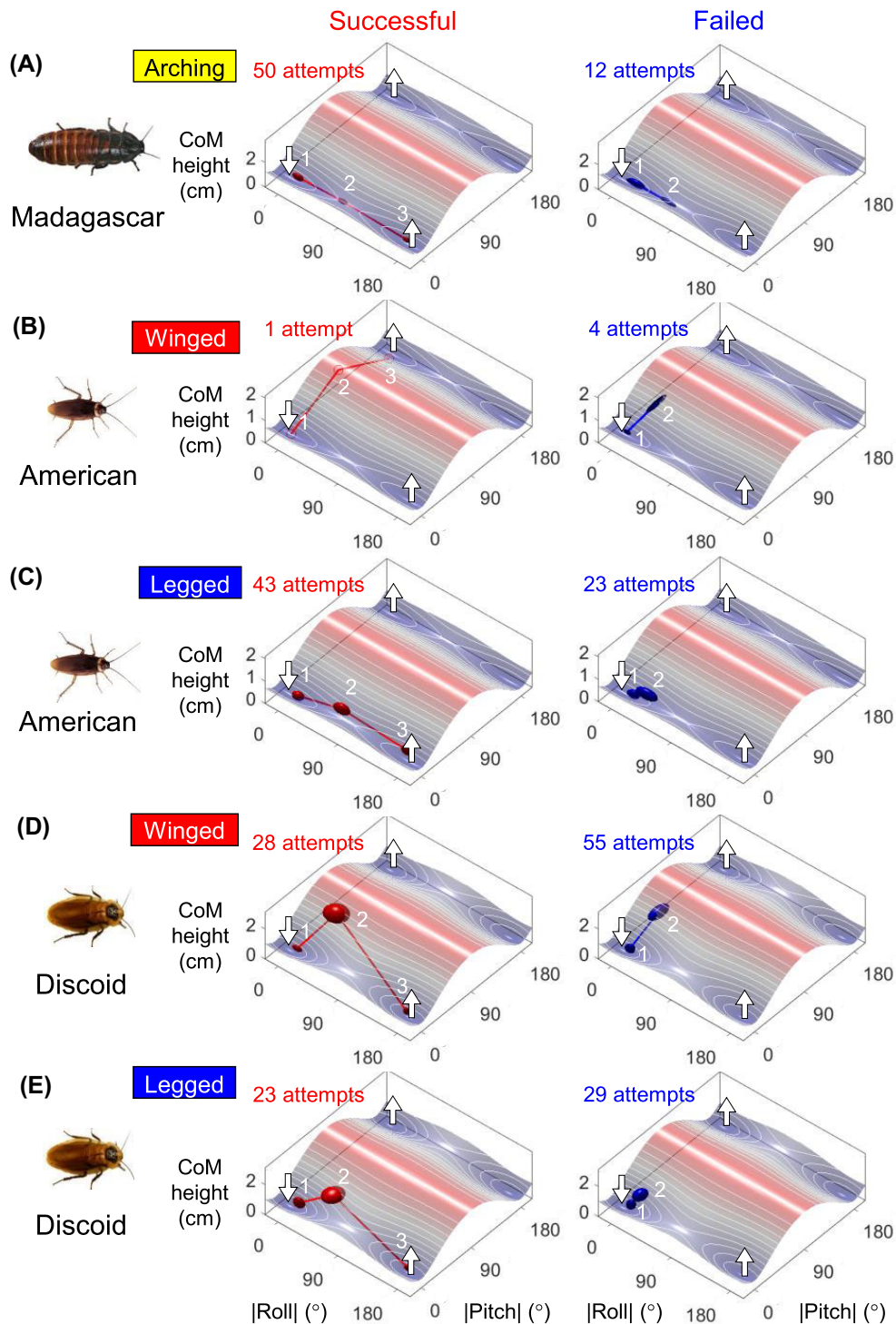
Fig. 8 State of the body on the potential energy landscape at the start (1), highest CoM position (2), and end (3) of the attempt during successful vs. failed attempts. (**A**) Madagascar hissing cockroach using body arching. (**B** and **C**) American cockroach using wings or legs. (**D**) Discoid cockroach using wings or legs. Potential energy landscape is defined in Fig. 5. On each landscape, the ellipsoids show means (center of ellipsoid) ± 1 standard deviation (principal semi-axis lengths of ellipsoid) of body pitch, body roll, and CoM height at each stage of the attempt. For failed attempts (right), the end state (3) is not shown because it nearly overlaps with the start state (1). The number of attempts of each case is shown. Adapted from Li et al. (2019).

energy landscape to assess how it rotates and how this affects the potential energy barrier (Fig. 8) (Li et al. 2019). For the Madagascar hissing cockroach using body arching, body rotation is mainly rolling (Figs. 8A and 5A), which overcomes the lowest potential energy barrier when successful. For the American cockroach using wings, body rotation is mainly pitching (Figs. 8B and 5B), which overcomes the highest barrier when successful. For the American cockroach using legs, body rotation is mainly rolling with a small amount of pitching (Figs. 8C and 5C), which overcomes nearly the lowest potential energy barrier when successful. By contrast, for the discoid cockroach using both wings and legs, body rotation has both large pitching and large rolling (Figs. 8D and E and 5D and E), which overcomes an intermediate potential energy barrier if successful. In addition, each species' body rotation is stereotyped, reaching a similar orientation when CoM is highest, whether the attempt is successful or not (Fig. 8A–E, small variation of state 2 orientation). This stereotypy suggests that physical constraints strongly confine the body rotation (Berman 2018). All three species also often have large body translation and yawing in the horizontal plane from appendage interaction with the level, flat, solid, low friction ground, but this does not contribute to self-righting as it cannot raise the CoM.

Cockroaches roll more in successful attempts

All three species roll their bodies more during successful self-righting attempts than in failed ones (Fig. 8, left vs. right) (Li et al. 2019). The higher body rolling in successful attempts lowers the potential energy barrier (Fig. 7B and C), making it easier to be overcome to achieve self-righting, given the mechanical energy that can be generated. Consistent with this finding, in our experiments using the initial robot (Fig. 1D), we also tested opening the two wings asymmetrically, where we found that with the more the body rolls the more likely the robot is to self-right (Li et al. 2016, 2017).

Ground self-righting is strenuous for cockroaches

However, for all three species using the strategies that lead to success, the increase in CoM height from the start to the highest CoM orientation (Fig. 8, from state 1 to state 2) is only slightly larger during successful attempts than in failed ones (Fig. 8, left vs. right) (Li et al. 2019). In other words, only a small difference in how much an animal can raise its CoM determines whether it succeeds or fails in overcoming the potential energy barrier. This, together with the observation that they often require multiple attempts to succeed (Fig. 4B), provides evidence that ground self-righting is strenuous for

these cockroaches: They can barely do enough work during each attempt to overcome the potential energy barrier (Othayoth et al. 2021). Previous force measurements also support this notion: for the discoid cockroach to self-right using legs, a single hind leg needs to generate a ground reaction force as large as eight times that during high-speed running (Full et al. 1995).

Strenuous, leg-assisted winged self-righting as a model system to study new questions

Our animal observations quantified stochastic yet stereotyped behavioral transitions and often complex yet stereotyped 3D body rotations, and our simplistic model explained why successful attempts have more body rolling. However, some new questions arose. First, why are the body rotations stereotyped, even though any arbitrary 3D rotations in the body pitch and roll space are in principle possible? Second, are the perturbing motions that accompany the motions of propelling appendages useful? Third, is the substantial randomness in the motions beneficial?

To further understand these, we performed three additional studies (Xuan and Li 2020a, 2020b; Othayoth and Li 2021), focusing on a model system—the discoid cockroach's strenuous, leg-assisted winged self-righting (Li et al. 2019) (Fig. 9). In this strategy, the overturned animal always first opens and pushes its wings against the ground to pitch up the body (Fig. 9A and B, blue). Because the two wings open together, the CoM falls within a triangular base of support formed by the two opened wings and head (Fig. 10A, black dashed triangle) (Othayoth and Li 2021). This intermediate state is metastable (i.e., stable provided that it is subjected to only small perturbations [Bovier and Den Hollander 2016]). However, wing pushing rarely pitches the animal sufficiently to complete a full somersault (Fig. 9A and B, dashed blue arrow), and the animal often continually attempts wing pushing but fails to self-right (Fig. 9A and B, solid blue arrows). When it eventually succeeds, the animal almost always rolls sideways over one of the wings from the metastable state (Fig. 9A and B, red arrow). Throughout this process, the animal often vigorously flails its legs in the air (Fig. 10A, red dashed curves). The legs also sometimes scrape the ground, the abdomen flexes and twists, and the wings often deform passively under load. All these motions, which have substantial randomness, may result in perturbations in the roll direction.

Specifically, for this model system, we need to answer the following three questions. First, why is the discoid cockroach's body rotation not mainly rolling, which has the lowest potential energy barrier, but instead first pitching then rolling when successful?
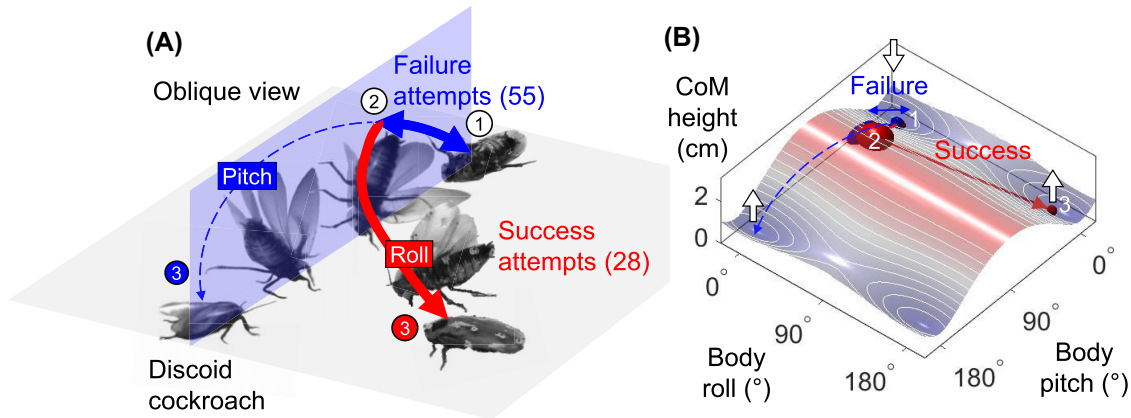
Fig. 9 Strenuous leg-assisted, winged self-righting of discoid cockroach as a model system. (**A**) Representative snapshots of the animal, illustrating body rotations during failed pitching attempts (thick blue arrows), a successful attempt by pure pitching (thin dashed blue arrow), and a successful attempt by pitching up first then rolling (red arrow). Adapted from Othayoth and Li (2021). (**B**) Stereotyped body rotation observed in successful (red) and failed (blue) attempts, overlaid on the potential energy landscape. In (A) and (B), 1, 2, and 3 show upside-down (1), metastable (2), and upright (3) states. This plot is the same as Fig. 8D, left and right merged, except that the axes are flipped to show the three stages' trajectory in a similar view as in Fig. 9A. See Fig. 8 for definition of elements.

Second, is the leg flailing motion that accompanies the wing opening motion useful? Third, is the substantial randomness in the coordination of the wing and leg motions beneficial?

Refined robophysical model of strenuous leg-assisted winged self-righting

To address these questions, we first created a refined robot as a robophysical model of strenuous, leg-assisted winged self-righting, following biological observations (Fig. 10A and B) (Othayoth and Li 2021). This robot is not aimed to achieve self-righting; that has already been done by the previous robot (Fig. 1D). Instead, we deliberately designed and controlled this robot to achieve similar *strenuous* self-righting behavior as the discoid cockroach's (Fig. 9A). Like the discoid cockroach (Fig. 10A), the refined robot has a head protruding forward from the body, creating the triangular metastable state (Fig. 10B, black dashed triangle), which the initial robot lacks. In addition, we limited the refined robot's wing opening amplitude so that it cannot self-right via pure body pitching. These make it a biologically relevant robophysical model for studying this strenuous strategy.

Robophysical modeling allows systematic parameter variation to discover physical principles of locomotion involving complex motions and locomotor–environment interactions (Aguilar et al. 2016). For leg-assisted winged self-righting, we need to systematically vary propelling wing motion and perturbing leg motion. To generate wing motion similar to that of the discoid cockroach, the refined robot opens both wings symmetrically, rolling and pitching them about the body by the same angle θ_{wing} (Fig. 10C and D, blue

arrows) to propel against the ground. Because the animal's perturbing motions are highly complex, to simplify parameter variation in the robot, we focused on the more frequent leg flailing. We chose to use a one degree-of-freedom, pendulum-like "leg," which oscillates laterally by the same amplitude to both sides, to generate perturbation (Fig. 10B, red arrow). Besides having similar geometric proportions to the animal (Fig. 10B vs. A), we also verified that the robot's leg actuation generated dynamically similar motion as that of the animal (Othayoth and Li 2021).

By opening and closing its wings repeatedly while oscillating the leg, the refined robot generates similar strenuous self-righting attempts, with similar motions as observed in the animal, not being able to self-right by pure body pitching, and often requiring multiple attempts to self-right via body rolling after first pitching up to the metastable state (e.g., Fig. 10E).

Propelling and perturbing appendages together enable barrier-crossing to self-right

In our experiments, we used the refined robot to measure the full 3D body rotation and wing motion during entire self-righting trials, which is challenging to measure for the animals due to the frequent occlusions (Li et al. 2019). This enabled us to reconstruct an accurate, "evolving" potential energy landscape, which changes with wing opening and closing, rather than the simplistic, fixed landscape from a rigid body (Figs. 7–9). We used this evolving potential energy landscape to understand how the propelling motion of the wings and perturbing motion of the leg together allow overcoming the
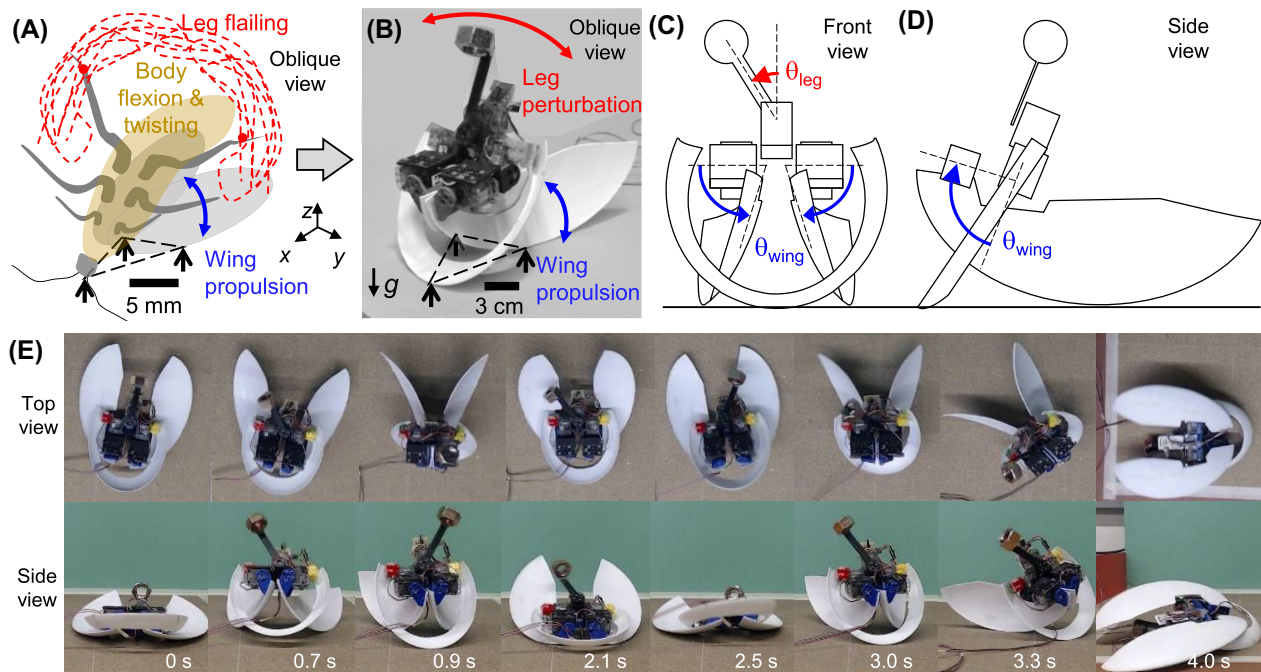
Fig. 10 Robophysical modeling of strenuous leg-assisted, winged self-righting. (A) Schematic of animal in metastable state. Blue arrows show wing opening (and closing) to propel against the ground. Red dashed curves show vigorous leg flailing. x– y– z is lab frame. (B) Refined robot in metastable state. In (A) and (B), dashed black triangle shows base of support, formed by ground contacts of head and two wing wedges. (C and D) Front and side view schematics of robot in metastable state to define leg angle θ_{leg} (red) and wing angle θ_{wing} (blue). Both wings rotate simultaneously. Each wing pitches away from the body (D) as well as rolls (E) to open. At any moment during wing opening and closing, wing pitching and rolling always reach the same angle θ_{wing}. (E) Representative snapshots of robot self-righting after two attempts. (A–D) are adapted from Othayoth and Li (2021). (E) is adapted from Xuan and Li (2020b).

potential energy barrier to self-right (Fig. 11) (Othayoth and Li 2021).

The potential energy landscape changes with wing angle θ_{wing} as the wings open and close (Fig. 11A and B). To self-right, the system has to escape from a metastable stability basin on the evolving potential energy landscape (Fig. 11B, ii, iii, white dot) and cross a potential energy barrier to reach one of several possible upright basins (Fig. 11B, upward white arrows). When the wings are closed (Fig. 11A, i), the robot is trapped in an upside-down basin (Fig. 11B, i, downward white arrow). As the wings open (Fig. 11A, ii), the upside-down basin shrinks to a metastable basin (Fig. 11B, ii, black arrow), which corresponds to the metastable state with a triangular base of support (Fig. 10B, black dashed triangle). As the wings continue to open (Fig. 11A, iii), the metastable basin becomes higher and moves closer (Fig. 11B, iii, black arrow) to the maximal potential energy barrier (Fig. 11B, black dashed line), which occurs for pure body pitching.

The increasing height of the metastable basin effectively reduces the pitch barrier (Fig. 11C, solid blue; pitch barrier is measured using the blue translucent planes in Fig. 11B) that can be overcome probabilisti-

cally by kinetic energy gained along the pitch direction when wing opening stops. However, because the refined robot's self-righting is strenuous by design, even at the maximal wing opening tested, the robot cannot gain enough kinetic energy along the pitch direction to cross the pitch barrier (Fig. 11C, blue, dashed vs. solid in the gray band) to reach the pitch upright basin (Fig. 11B, upward white arrow labeled by blue circle 3), i.e., it cannot self-right by pure pitching (Fig. 11A, top leftmost). Thus, it is trapped in metastable basin, when there are no leg oscillations to inject kinetic energy along the roll direction (Fig. 11D, black, failure trajectories).

However, wing opening also reduces the barrier along the roll direction (Fig. 11C, solid red; roll barrier is measured using the red translucent planes in Fig. 11B). This allows the small kinetic energy along the roll direction from perturbing leg oscillations to overcome the roll barrier probabilistically (Fig. 11C, red, dashed vs. solid in the gray band). Thus, the robot can reach the upright roll basin (Fig. 11B, iii, red arrow, reaching the upward white arrow labeled by red circle 3), i.e., it self-rights by rolling after pitching (Fig. 11A, bottom leftmost), when there are sufficient leg oscillations (Fig. 11D, white, success trajectories). As a result, the larger
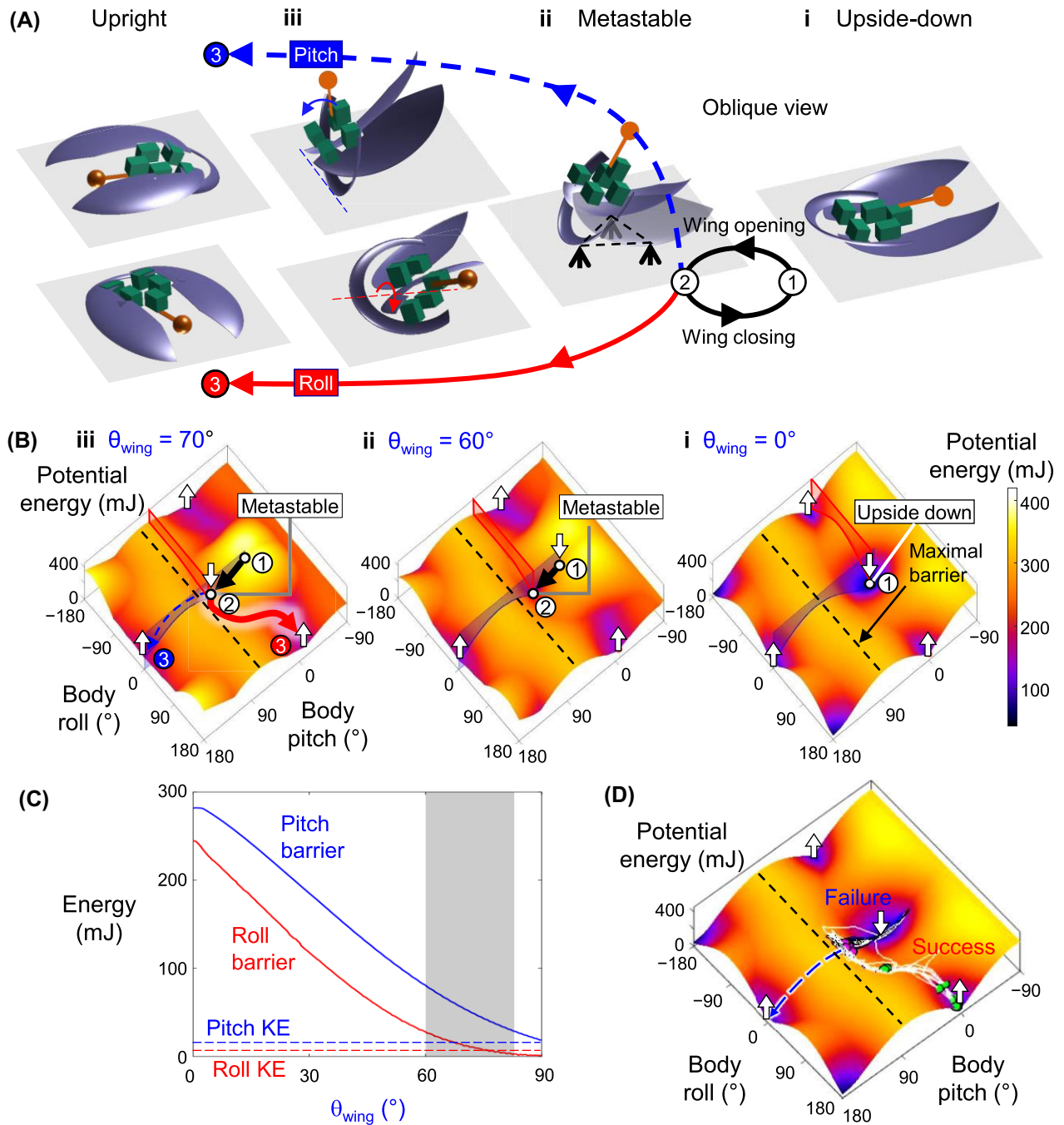
Fig. 11 Refined robot's self-righting motion and evolving potential energy landscape. (**A**) From right to left: schematic of robophysical model in (i) upside-down and (ii) metastable states, and (iii) self-righting by pure pitching (top) and pitching then rolling (bottom). The top and bottom cases correspond to the observed successful and failed attempts in Fig. 9B. (**B**) Corresponding evolving potential energy landscape at different wing opening angles θ_{wing}. 1–3 show upside-down (1), metastable (2), and upright (3) states. Translucent blue and red cross-sectional cuts through the upside-down or metastable local minimum along the pitch and roll axes are used to quantify pitch and roll potential energy barrier. (**C**) Pitch (blue) and roll (red) potential energy barrier as a function of wing opening angle θ_{wing}. Blue and red dashed lines show average maximal pitch and roll kinetic energy, respectively. Gray band shows range of wing opening amplitudes Θ_{wing} tested for this robophysical model. (**D**) Ensemble of system state trajectories from all the trials with a given wing opening magnitude. Black: failure to self-right by pure pitching, but being attracted to and trapped in metastable basin. White: successfully self-righting by pitching, then rolling. Adapted from Othayoth and Li (2021).

the robot leg oscillation makes self-righting more probable and reduces the number of attempts required.

Besides flailing legs that we modeled, other perturbing motions observed in the animal likely also contribute to self-righting. For example, small forces from legs scraping the ground (Li et al. 2019) may also inject roll kinetic energy. Abdominal flexion and twisting and passive wing deformation under load (Li et al. 2019) should tilt the potential energy landscape toward one side and lower the roll barrier on that side. Both these effects should make self-righting easier.

Stereotyped body rotation results from physical constraints

When the reconstructed robot rotation trajectories are visualized on the landscape, it is clear that the physical interaction with the ground, which is modeled by a stochastic, self-propelled system with kinetic energy moving on the potential energy landscape, strongly constrains the stochastic system's behavior, resulting in a stereotyped ensemble of trajectories for both successful and failed attempts (Fig. 11D) (Othayoth and Li 2021). This suggested that the discoid cockroach's stereotyped body rotation is largely a result of the physical constraint, consistent with previous findings that physical constraints lead to stereotyped legged locomotion on level, flat, solid ground (Berman 2018).

Robot simulation to study effect of substantial randomness in appendage coordination

Next, we studied the third question—whether the substantial randomness in the coordination of the wing and leg motions is beneficial. To do so, we first created a multi-body dynamics simulation of the refined robot (Fig. 12A) (Xuan and Li 2020b). After being validated against the physical robot experiments (Fig. 10E, see more detail in Xuan and Li 2020b), the robot simulation allowed us to control and vary the level of motion randomness systematically and collect a large number of trials required to understand its impact, which is less practical in the physical robot and impossible in the animal.

Substantial randomness in appendage coordination increases self-righting probability

Our simulation study revealed that a substantial level of randomness in the motions allows the system to find good coordination between propelling and perturbing appendages, which is more likely to lead to successful self-righting (Xuan and Li 2020b). We measured the levels of randomness in the discoid cockroach's wing opening/closing and leg oscillation periods (Fig. 12B). They are substantially higher than that of the highly rhythmic leg oscillations during walking (Watson and Ritzmann 1997) and running (Full and Tu 1990). This substantial level of randomness in both wing and leg oscillation periods results in substantial level of randomness in the phase offset between these two oscillations. Thus, to study the effect of randomness, in the robot simulation, we added Gaussian noise to the time delay between wing and leg oscillations (see definition in Fig. 12C), which injects a similar level of randomness to the coordination (phase offset) between them. When wing opening magnitude Θ_{wing} and leg oscillation magnitude Θ_{leg} are small (representing an animal that is too tired), self-righting always fails, whether there is substantial randomness or not (Fig. 12D and E, top left regions). When Θ_{wing} and Θ_{leg} are large (representing an animal that is very energetic), self-righting always succeeds, whether there is substantial randomness or not (Fig. 12D and E, bottom right regions). However, for intermediate Θ_{wing} and Θ_{leg}, when the robot can nearly overcome the potential energy barrier, the substantial randomness increases self-righting probability from 0 to >40% (Fig. 12D vs. E, critical regime). Because ground self-righting is so strenuous that the animal often barely overcomes the barrier, this finding suggests that the substantial randomness observed in the animals is beneficial to them.

Substantial randomness helps find good coordination that leads to success

Further simulation revealed why substantial randomness in the coordination between propelling wings and perturbing legs increases self-righting probability (Xuan and Li 2020b). The leg-wing phase offset has a direct impact on self-righting outcome: good phase offsets almost always lead to success (Fig. 12F and G, white), whereas bad phase offsets almost always lead to failure (Fig. 12F and G, black). Thus, a substantial level of randomness in phase offset allows the system to explore various phase offsets, thereby increasing the chance of finding a good coordination between them that leads to successful self-righting (Fig. 12G, yellow arrows), whereas strictly periodic motions with no randomness traps the system in bad phase offsets always resulting in failure (Fig. 12F, yellow arrows).

Template to understand why appendage coordination affects self-righting outcome

Finally, to understand why a substantial level of randomness is useful, we created a template model of strenuous, leg-assisted winged self-righting (Fig. 13B) (Xuan and Li 2020a). A template is the simplest
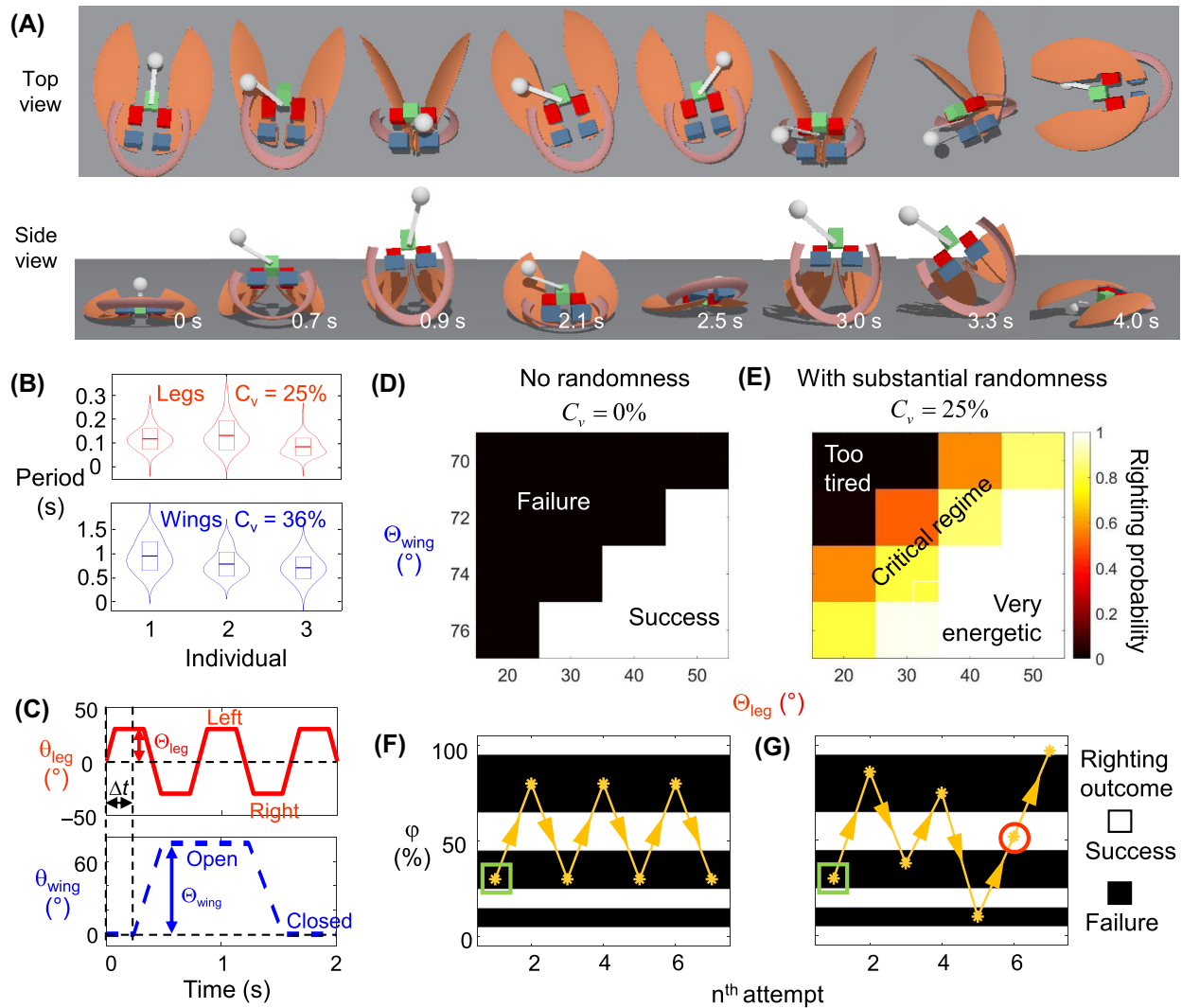
Fig. 12 Robot simulation reveals benefit of substantial randomness in appendage coordination. (**A**) Representative snapshots of simulation robot self-righting after two attempts. Note the resemblance to the refined robot experiments in Fig. 10E. (**B**) Violin plots of wing opening/closing and leg oscillation periods for three discoid cockroach individuals. Inner rectangle shows mean $\pm$ 1 standard deviation. The level of randomness is measured by coefficient of variation, C_v = standard deviation/mean. (**C**) Actuation profiles of wings (blue) and leg (red) angles (see definition in Fig. 10C and D) of simulation robot. Θ_{wing} and Θ_{leg} are wing opening amplitude and leg oscillation amplitude, respectively. Δt is the time delay, defined as the time interval between the start of wing opening and the start of the preceding leg oscillation. Gaussian noise δt is added to Δt in simulation to introduce randomness in phase offset between wing and leg oscillations for each cycle, which can be varied to change the overall randomness level (measured by C_v). (**D** and **E**) Self-righting probability of the simulated robot as a function of Θ_{wing} and Θ_{leg}, comparing without ($C_v = 0$) and with substantial ($C_v = 25\%$) randomness in wing-leg coordination (phase offset). (**F** and **G**) Evolution of phase offset φ over consecutive attempts (yellow points connected by arrows), overlaid on phase offset map (white: good phase offsets resulting in successful self-righting, black: bad phase offsets leading to failure), comparing without ($C_v = 0$) and with substantial ($C_v = 25\%$) randomness. Green box shows initial phase offset at the first attempt. Red circle shows the first good phase offset reached with substantial randomness, resulting in success. Adapted from Xuan and Li (2020b).

analytical model, comprised of the fewest components and degrees of freedom, that captures fundamental dynamics of this self-righting behavior (Full and Koditschek 1999). Because successful winged self-righting almost always occurs eventually via rolling in both the discoid cockroach (Fig. 9B) and the refined

robot (Figs. 10E, 11D, and 12A), our 2D template models the planar rolling dynamics of self-righting and trims away the complexity of the system (from Fig. 13A to B). This allowed writing down closed-form equations of motion that can be solved numerically to calculate the dynamics of the system.
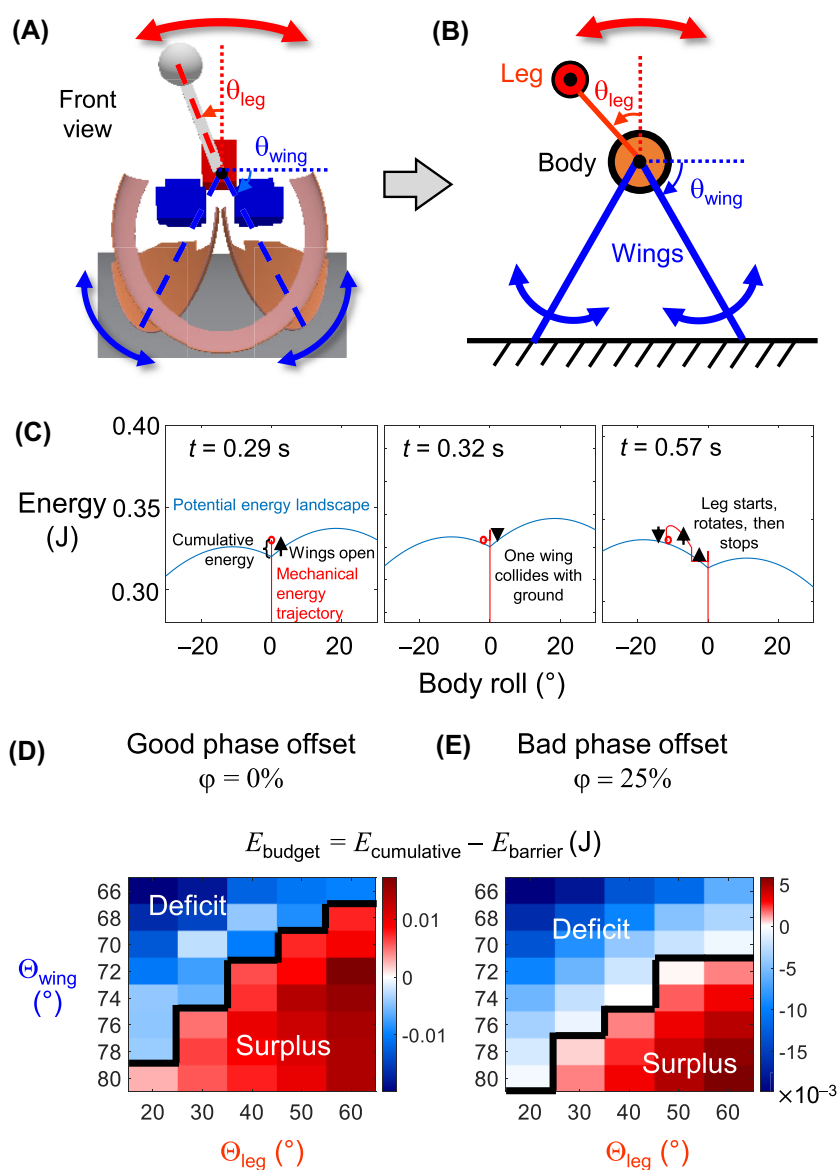
Fig. 13 Template model reveals why appendage coordination is important. (**A**) Front view of simulation robot in metastable state. (**B**) Template model capturing planar dynamics of the refined robot. Two point masses represent body (orange) and leg pendulum mass (red). Three massless links represent wings (blue segments) and leg linkage (red segment). In (**A** and **B**), blue and red arrows show wing opening/closing and leg oscillation, respectively. (**C**) Example snapshots of system cumulative mechanical energy (red dot) evolution (red trajectory) during a modeling trial, overlaid on evolving potential energy landscape over body roll (blue curve), calculated from the template model. Black bracket defines cumulative energy, the extra mechanical energy above that of the local minimum of the basin that the system is in. Left: as the wings open. Middle: As one wing collides with the ground. Right: as the leg starts, rotates, and stops. Small upward and downward arrows show cumulative energy increase and reduction in these processes. (**D** and **E**) Mechanical energy budget as a function of Θ_{wing} and Θ_{leg}, calculated from the template, comparing without ($C_v = 0$) and with substantial ($C_v = 25\%$) randomness in wing-leg coordination (phase offset). Mechanical energy budget is cumulative energy minus the potential energy barrier: $E_{budget} = E_{cumulative} - E_{barrier}$. The black boundaries separate two regions. The surplus region is where cumulative mechanical energy exceeds the potential energy barrier, leading to successful self-righting. The deficit region is where cumulative mechanical energy is insufficient to overcome the potential energy barrier, resulting in failure. Adapted from Xuan and Li (2020a).

Good appendage coordination accumulates more energy to overcome barrier

Successful self-righting requires cumulating sufficient mechanical energy (potential energy and kinetic energy) to overcome the potential energy barrier (which

is not always fixed but can be lowered). Thus, to further understand why phase offset affects self-righting outcomes, we used the template model to calculate the system's cumulative energy and barrier, compare whether there is sufficient cumulative energy to

overcome the barrier (i.e., mechanical energy budget), and assess how phase offset affects this mechanical energy budget (Xuan and Li 2020a).

We calculated the evolving potential energy landscape (potential energy as a function of body roll) of the template model (e.g., Fig. 13C, blue) to obtain the potential energy barrier $E_{barrier}$. We calculated how the system's mechanical energy changes during self-righting attempts (e.g., Fig. 13C, red dot and trajectory) to obtain cumulative energy $E_{cumulative}$, defined as the system's extra mechanical energy above the potential energy of the local minimum of the basin that the system is in (Fig. 13C, left, black bracket). Cumulative energy changes over each actuation phase or collision event: it increases or decreases as the wings open or close (e.g., Fig. 13C, left), increases or decreases as the legs oscillate (e.g., Fig. 13C, right), and always decreases as the robot collides with the ground (e.g., Fig. 13C, middle).

We then used the template model to assess mechanical energy budget, $E_{cumulative} - E_{barrier}$, i.e., whether cumulative energy exceeds the potential energy barrier, over a broad range of wing opening and leg oscillation amplitudes, comparing between good and bad phase offsets (e.g., Fig. 13D vs. E) (Xuan and Li 2020a). For both good and bad phase offsets, there is an increasing energy budget surplus as Θ_{wing} and Θ_{leg} increase (Fig. 13D and E, red regions), and there is an increasing energy deficit as Θ_{wing} and Θ_{leg} decrease (Fig. 13D and E, blue regions). However, phase offset strongly affects self-righting outcomes by changing mechanical energy budget. Well-coordinated appendage motions with good phase offsets accumulate more mechanical energy than poorly-coordinated ones with bad phase offsets, thereby more effectively overcoming the potential energy barrier (i.e., having a larger energy surplus) and thus self-righting more successfully. Together with the insight that substantial randomness helps find good phase offsets (Fig. 12F and G), this explains why higher randomness increases self-righting probability (Fig. 12D vs. E).

Summary

We performed the first studies of biological ground self-righting in three dimensions, using three species of cockroaches. For all three species, ground self-righting is strenuous and may require multiple attempts to succeed (Fig. 4). Two of the three species often self-right dynamically, by generating substantial pitch and/or roll kinetic energy to overcome the potential energy barrier. Each species uses multiple strategies and displays stochastic yet stereotyped transitions across them (Figs. 5 and 6). The propelling motion from primary appendages is often accompanied by perturbing motions from other appendages, and all these motions have substantial randomness. Body rotations are complex yet stereotyped (Fig. 8). Compared to failed attempts, in successful attempts their body rolls more, which lowers the potential energy barrier (Fig. 8).

We combined robophysical, simulation, and template modeling to understand the physical principles of ground self-righting. Our experiments using an initial robot as a robophysical model revealed that, when propelling against the ground to generate simple planar rotation, the longer and faster appendages push, the more mechanical energy can be gained to overcome the barrier, and thus the more likely and faster self-righting is (Fig. 3). However, the animals can rarely achieve this, because of how strenuous self-righting is for them. To understand the physical principles of strenuous self-righting, we further studied the discoid cockroach's leg-assisted winged self-righting as a model system (Fig. 9). Our robophysical modeling using a refined robot (Fig. 10) revealed that propelling (e.g., wings) or perturbing (e.g., legs) appendages alone cannot gain enough kinetic energy to overcome the high potential energy barrier (Fig. 11). However, when used together, the propelling motion reduces the barrier sufficiently so that it can be overcome probabilistically by the small kinetic energy from perturbing motion (Fig. 11). Thus, only by combining propelling and perturbing motions can self-righting be achieved, when it is so strenuous; this physical constraint (Fig. 11D) leads to the stereotyped body rotation (Fig. 9B). Our robot simulation and template modeling revealed that the substantial randomness observed in the propelling and perturbing motions helps find good coordination between them (Fig. 12), which accumulates more mechanical energy to overcome the potential energy barrier (Fig. 13), thus increasing the likelihood of self-righting.

Future work

Further experiments using more species and more elaborate ("anchor"-level [Full and Koditschek 1999]) models that better capture the biological detail are needed to generalize the physical principles to diverse biological morphologies and behavior (as well as diverse robot design and actuation). In particular, how limbless and elongate animals (Hu and Shelley 2012) self-right on the ground (and even in the air), and how similar robots should do so, remain to be explored. The use of distributed force plates (Dai et al. 2011) to measure ground reaction forces generated by multiple appendages and body deformation will facilitate this progress. In addition, our findings suggest that animals may use sensory feedback to actively adjust their strategy and appendage motions and body deformation to better self-

right, which should be tested by future neurophysiological studies.

Given our progress, the physical principles of ground self-righting in complex terrains remain poorly understood. Natural terrains are rarely perfectly level, flat, solid, and with low friction throughout, can be flowable (Li et al. 2013), and can have random objects to grasp onto. Recent animal studies have begun to observe and quantify ground self-righting behavior on surfaces of various roughness (Sasaki and Nonaka 2016; Pace and Harris 2021; Zhang et al. 2021; Bien et al. 2024) and unevenness (Sasaki and Nonaka 2016; Zhang et al. 2021), that are flowable (Pace and Harris 2021), or with objects nearby (Sasaki and Nonaka 2016). Rougher or uneven surfaces and random nearby objects facilitate self-righting, and animals adjust their use of diverse strategies correspondingly (Sasaki and Nonaka 2016; Pace and Harris 2021; Zhang et al. 2021; Bien et al. 2024). In light of these studies, the level, flat, solid, low friction ground used in our studies is likely among the challenging surfaces to self-right on. (It is noteworthy that, despite how strenuous ground self-righting is as our modeling revealed, all three species studied can almost always self-right with 30 s [Fig. 4A, white], underscoring the notion that ground self-righting is a crucial locomotor ability that almost all terrestrial animals must possess to survive.) Rougher surfaces likely allow animals to generate larger forces to pitch and/or roll the body to self-right. Similarly, uneven terrain may have asperities of the right sizes (Clifton et al. 2023) for appendages to interlock or even grasp onto to generate large self-righting forces and torques (Sasaki and Nonaka 2016). A sloped surface is presumably easier to self-right on, as animals may rotate on it to gain kinetic energy or slide down to encounter more favorable terrain features. Furthermore, the largely unsuccessful strategies or motions found here may be useful in complex terrains. For example, body twisting may allow legs to reach and grasp onto nearby objects, leg scraping may help engage asperities, and body yawing and sliding may help reach rougher and uneven parts of the terrain, all contributing to self-righting. However, due to their complex mechanics, it is unclear whether flowable substrates make self-righting more or less difficult without modeling the substrate forces (Li et al. 2013). Similarly, for marine animals on the bottom substrates (Silvey and Silvey 1973; Weldon and Hoffman 1979; Hoffman 1980; Young et al. 2006; Zhang et al. 2020), how hydrostatic and hydrodynamic forces work together with substrate forces to achieve underwater ground self-righting is unknown. Future work should measure and model ground self-righting in more complex terrains in three dimensions to elucidate broader physical principles. Our quantitative experimental and modeling approaches demonstrated here will facilitate this progress.

Acknowledgments

Funding

Conflict of interest

I have no conflict of interest.

Data availability

The data reviewed in this article are available in the original research articles cited and their online supplementary materials.

References

Aguilar J, Zhang T, Qian F, Kingsbury M, McInroe B, Mazouchova N, Li C, Maladen R, Gong C, Travers M et al. 2016. A review on locomotion robophysics: The study of movement at the intersection of robotics, soft matter and dynamical systems. Rep Prog Phys 79:110001.

Ashe VM. 1970. The righting reflex in turtles: A description and comparison. Psychon Sci 20:150–2.

Berman GJ. 2018. Measuring behavior across scales. BMC Biol 16:1–11.

Bien T, Alexander B, Li C, Goeler-Slough N, Hsieh ST, Kane SA. 2024. Using pose estimation and 3D rendered models to study leg-mediated self-righting by lanternflies. Integr Comp Biol:icae014. https://doi.org/10.1093/icb/icae014.

Bolmin O, Duan C, Urrutia L, Abdulla AM, Hazel AM, Alleyne M, Dunn AC, Wissa A. 2017. Pop! Observing and modeling the legless self-righting jumping mechanism of click beetles. Biomimetic and Biohybrid Systems: 6th International Conference, Living Machines 2017, Stanford, CA, USA, July 26–28, 2017, Proceedings. Vol. 6, 35–47, Cham: Springer.

Bovier A, Den Hollander F. 2016. Metastability: A potential-theoretic approach. Cham: Springer.

Brackenbury J. 1990. A novel method of self-righting in the springtail *Sminthurus viridis* (Insecta: Collembola). J Zool 222:117–9.

Brown AEX, de Bivort B. 2018. Ethology as a physical science. Nat Phys 14:653–7.

Camhi JM. 1977. Behavioral switching in cockroaches: transformations of tactile reflexes during righting behavior. J Comp Physiol 113:283–301.

Caporale JD, McInroe BW, Ning C, Libby T, Full RJ, Koditschek DE. 2020. Coronal plane spine twisting composes shape to adjust the energy landscape for grounded reorientation. 2020 IEEE International Conference on Robotics and Automation (ICRA), 8052–8.

Clifton G, Stark AY, Li C, Gravish N. 2023. The bumpy road ahead: The role of substrate roughness on animal walking and a proposed comparative metric. J Exp Biol 226: jeb245261.

Dai Z, Wang Z, Ji A. 2011. Dynamics of gecko locomotion: A force-measuring array to measure 3D reaction forces. J Exp Biol 214:703–8.

Davis WJ. 1968. Lobster righting responses and their neural control. Proc R Soc London Ser B Biol Sci 170: 435–56.

Domokos G, Várkonyi PL. 2008. Geometry and self-righting of turtles. Proc R Soc London B Biol Sci 275:11–7.

Evans MEG. 1972. The jump of the click beetle (Coleoptera, Elateridae)—A preliminary study. J Zool 167:319–36.

Ewart HE, Tickle PG, Sellers WI, Lambertz M, Crossley DA, Codd JR. 2022. The metabolic cost of turning right side up in the Mediterranean spur-thighed tortoise (*Testudo graeca*). Sci Rep 12:431.

Faisal AA, Matheson T. 2001. Coordinated righting behaviour in locusts. J Exp Biol 204:637–48.

Frantsevich L. 2004. Righting kinematics in beetles (Insecta: Coleoptera). Arthropod Struct Dev 33:221–35.

Frantsevich L, Mokrushov PA. 1980. Turning and righting in geotrupes (Coleoptera, Scarabaeidae). J Comp Physiol 136:279–89.

Full RJ, Tu MS. 1990. Mechanics of six-legged runners. J Exp Biol 146:129–46.

Full RJ, Yamauchi A, Jindrich D. 1995. Maximum single leg force production: cockroaches righting on photoelastic gelatin. J Exp Biol 198:2441–52.

Full RJ, Koditschek DE, 1999. Templates and anchors: neuromechanical hypotheses of legged locomotion on land. J Exp Biol 202:3325–32.

Golubović A, Tomović L, Ivanović A. 2015. Geometry of self righting: the case of Hermann's tortoises. Zool Anzeiger—A J Comp Zool 254:99–105.

Graham D. 1979. Effects of circum-oesophageal lesion on the behaviour of the stick insect *Carausius morosus*. Biol Cybernetics 32:139–45.

Hoffman D. 1980. Defensive responses of marine gastropods (Prosobranchia, Trochidae) to certain predatory seastars and the dire whelk, Searlesia Dira (Reeve). Pacific Science 34:233–43.

Hu DL, Shelley M. 2012. Slithering locomotion. In: Childress S, Hosoi A, Schultz WW, Wang ZJ, editor. Natural locomotion in fluids. New York: Springer, Vol. 155, 117–35.

Jusufi A, Goldman DI, Revzen S, Full RJ. 2008. Active tails enhance arboreal acrobatics in geckos. Proc Natl Acad Sci USA 105:4215–9.

Kessens CC, Smith DC, Osteen PR. 2012. A framework for autonomous self-righting of a generic robot on sloped planar surfaces. 2012 IEEE International Conference on Robotics and Automation, 4724–9.

Koppányi T, Kleitman N. 1927. Body righting and related phenomena in the domestic duck (*Anas boscas*). Am J Physiol Legacy Content 82:672–85.

Li C, Pullin AO, Haldane DW, Lam HK, Fearing RS, Full RJ. 2015. Terradynamically streamlined shapes in animals and robots enhance traversability through densely cluttered terrain. Bioinspir Biomim 10:046003.

Li C, Kessens CC, Fearing RS, Full RJ. 2017. Mechanical principles of dynamic terrestrial self-righting using wings. Adv Robot 31:881–900.

Li C, Kessens CC, Young A, Fearing RS, Full RJ. 2016. Cockroach-inspired winged robot reveals principles of ground-based dynamic self-righting. 2016 IEEE/RSJ International Conference on Intelligent Robots and Systems (IROS), 2128–34.

Li C, Wöhrl T, Lam HK, Full RJ. 2019. Cockroaches use diverse strategies to self-right on the ground. J Exp Biol 222: jeb186080.

Li C, Zhang T, Goldman DI. 2013. A terradynamics of legged locomotion on granular media. Science 339:1408–12.

Malashichev Y. 2016. Asymmetry of righting reflexes in sea turtles and its behavioral correlates. Physiol Behav 157:1–8.

Mann GKH, O'Riain MJ, Hofmeyr MD. 2006. Shaping up to fight: sexual selection influences body shape and size in the fighting tortoise (*Chersina angulata*). J Zool 269:373–9.

Ortega-Jimenez VM, Jusufi A, Brown CE, Zeng Y, Kumar S, Siddall R, Kim B, Challita EJ, Pavlik Z, Priess M et al. 2023. Air-to-land transitions: from wingless animals and plant seeds to shuttlecocks and bio-inspired robots. Bioinspir Biomim 18:051001.

Othayoth R, Li C. 2021. Propelling and perturbing appendages together facilitate strenuous ground self-righting. eLife 10:e60233.

Othayoth R, Xuan Q, Wang Y, Li C. 2021. Locomotor transitions in the potential energy landscape-dominated regime. Proc Biol Sci 288:20202734.

Pace CM, Harris M. 2021. Flat on its back: the impact of substrate on righting methods of the brown marmorated stink bug, *Halyomorpha Halys*. J Comp Physiol A 207:747–55.

Pellis VC, Pellis SM, Teitelbaum P. 1991. A descriptive analysis of the postnatal development of contact-righting in rats (*Rattus norvegicus*). Dev Psychobiol 24:237–63.

Reingold SC, Camhi JM. 1977. A quantitative analysis of rhythmic leg movements during three different behaviors in the cockroach, *Periplaneta americana*. J Insect Physiol 23:1407–20.

Robins A, Lippolis G, Bisazza A, Vallortigara G, Rogers LJ. 1998. Lateralized agonistic responses and hindlimb use in toads. Anim Behav 56:875–81.

Rubin AM, Blob RW, Mayerl CJ. 2018. Biomechanical factors influencing successful self-righting in the pleurodire turtle *Emydura subglobosa*. J Exp Biol 221:jeb182642.

Sasaki M, Nonaka T. 2016. The reciprocity of environment and action in self-righting beetles: the textures of the ground and an object, and the claws. Ecol Psychol 28:78–107.

Sherman E, Novotny M, Camhi JM. 1977. A modified walking rhythm employed during righting behavior in the cockroach *Gromphadorhina portentosa*. J Comp Physiol 113:303–16.

Silvey GE, 1973. Motor control of tail spine rotation of the horseshoe crab, *Limulus polyphemus*. J Exp Biol 58:599–625.

Stancher G, Clara E, Regolin L, Vallortigara G. 2006. Lateralized righting behavior in the tortoise (*Testudo hermanni*). Behav Brain Res 173:315–9.

Várkonyi PL, Domokos G. 2006. Mono-monostatic bodies: the answer to Arnold's question. Math Intell 28:34–8.

Vince MA. 1986. Response of the newly born Clun Forest lamb to maternal vocalisations. Behaviour 96:164–70.

Watson JT, Ritzmann RE. 1997. Leg kinematics and muscle activity during treadmill running in the cockroach, *Blaberus discoidalis*: I. Slow running. J Comp Physiol A 182:11–22.

Weldon PJ, Hoffman DL. 1979. Kick and thrust foot movements in the righting and escape behavior of marine prosobranch gastropods (Mollusca: Gastropoda). Z Tierpsychol 50:387–98.

Willemsen RE, Hailey A. 2003. Sexual dimorphism of body size and shell shape in *European tortoises*. J Zool Lond 260:353–65.

Xuan Q, Li C. 2020a. Coordinated appendages accumulate more energy to self-right on the ground. IEEE Robot Autom Lett 5:6137–44.

Xuan Q, Li C. 2020b. Randomness in appendage coordination facilitates strenuous ground self-righting. Bioinspir Biomim 15:065004.

Young JS, Peck LS, Matheson T. 2006. The effects of temperature on walking and righting in temperate and Antarctic crustaceans. Polar Biol 29:978–87.

Zeng Y, Lam K, Chen Y, Gong M, Xu Z, Dudley R. 2017. Biomechanics of aerial righting in wingless nymphal stick insects. Interface Focus 7:20160075.

Zhang J, Li J, Li C, Wu Z, Liang H, Wu J. 2021. Self-righting physiology of the ladybird beetle *Coccinella septempunctata* on surfaces with variable roughness. J Insect Physiol 130:104202.

Zhang Y, Li S, Zuo P, Li J, Liu J. 2020. A mechanics study on the self-righting of abalone from the substrate. Appl Bionics Biomech 2020:8825451.

Zill SN. 1986. A model of pattern generation of cockroach walking reconsidered. J Neurobiol 17:317–28.